Azacalixphyrins as NIR photoacoustic contrast agents

Lucien Lavaud, Simon Pascal, Khaled Metwally, Damien Gasteau, Anabela da Silva, Zhongrui Chen, Mourad Elhabiri, Gabriel Canard, Denis Jacquemin, Olivier Siri

Azacalixphyrins as NIR Photoacoustic Contrast Agents

Lucien Lavaud,[a] Simon Pascal,*[a] Khaled Metwally,[b] Damien Gasteau,[b] Anabela Da Silva,*[b] Zhongrui Chen,[a] Mourad Elhabiri,[c] Gabriel Canard,[a] Denis Jacquemin[d] and Olivier Siri*[a]

[a.] *Aix-Marseille Université, CNRS UMR 7325, Centre Interdisciplinaire de Nanoscience de Marseille (CINaM), Campus de Luminy, 13288 Marseille cedex 09, France.*
[b.] *Aix Marseille Univ, CNRS, Centrale Marseille, Institut Fresnel, Marseille, France.*
[c.] *Université de Strasbourg, Université de Haute-Alsace, CNRS, LIMA, UMR 7042, Equipe Chimie Bioorganique et Médicinale, ECPM, 25 Rue Becquerel, 67000 Strasbourg, France.*
[d.] *Laboratoire CEISAM, CNRS UMR 6230, Université de Nantes, 2, rue de la Houssinière, 44322 Nantes, France.*
† Electronic Supplementary Information (ESI) available: experimental protocols, ^{1}H and ^{13}C NMR spectra, additional solvatochromism and pH-dependent absorption spectra, theoretical modelling. See DOI: 10.1039/x0xx00000x

Near-infrared (NIR) azacalixphyrins bearing aryl substituents strongly impacting the physico-chemical properties of the macrocycles were designed, enabling hyperchromic and bathochromic shifts of the absorption compared to the N-alkylated analogues. This engineering enhances the photoacoustic response under NIR excitation, making azacalixphyrins promising organic contrast agents that reach the 800-1000 nm range.

Photoacoustic imaging (PAI) is an emerging non-invasive method that enables the imaging of biological media of interest with an important contrast due to the excellent penetration of ultrasounds within tissues.[1] Photoacoustic microscopy is therefore particularly competitive compared to other methods based on fluorescence (confocal or two-photon microscopy) and has already proven its efficiency in the fields of vascular imaging and cancer characterization.[2] In fact, the enthusiasm in using this technique for biomedical sensing is growing since the 1990s, impacting several applications such as breast cancer detection,[3] small animal molecular imaging,[4] subcutaneous structures imaging,[5] and functional imaging.[6] While the first contrast materials used for PAI were mainly metallic nanoparticles (Au, Ag, Cu), the attention of the scientific community has turned to the development of organic chromophores.[7] Indeed, organic dyes offer several competitive assets: (i) potential low toxicity, (ii) possible vectorization in biological media through simple chemical modifications (solubility, size…), and (iii) tuneable optical properties (absorption region, de-excitation pathways…). This latter parameter is of crucial importance since the laser excitation of the chromophores is the most efficient within the near-infrared region (NIR), which includes the transparency window of biological media (*ca.* 700-1000 nm). Thus, far-red and NIR dyes with high molar absorptivity are particularly sought for PAI and recent investigations have shown that polymethine (cyanines, squaraines, BODIPYs, curcuminoids…)[8] or porphyrinoid (porphyrins, phthalocyanines…)[9] derivatives are very promising candidates. However, some drawbacks appeared from these examples, e.g., the fluorescence of these derivatives is detrimental for PAI. In addition, the maximum of absorption used for laser irradiation has been, so far, located in the 700-850 nm spectral range for organic dyes,[9] while excitation at lower energies would undoubtedly enhance the contrast (signal-to-noise ratio) due to better penetration of NIR light within tissues and biological media.

In this context, azacalixphyrins **1-3** (ACP, Fig 1) are prime candidates to overcome these important drawbacks because they are NIR absorbers and totally non-emissive chromophores. Furthermore, they can be easily engineered to modulate their optical properties and/or solubility.[10] Structurally, under their neutral state, ACPs are highly stable bis-zwitterionic scaffold constituted of a di-anionic aromatic macrocycle (18 π-electrons), and peripheral cationic trimethine units poorly conjugated with the aromatic core according to Dahne and Leupold's "coupling principle" in polymethine dyes.[11]

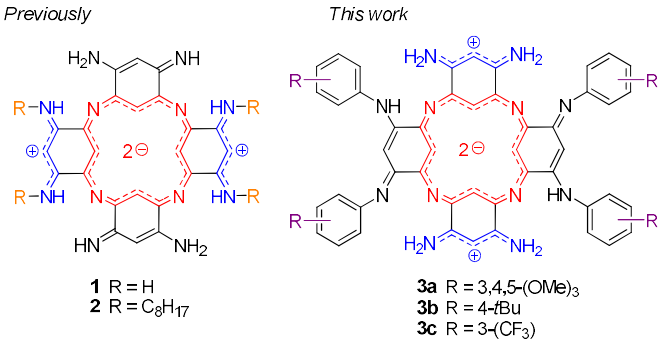

Fig. 1. Chemical structures of the neutral forms of alkyl and aryl *N*-substituted ACPs.

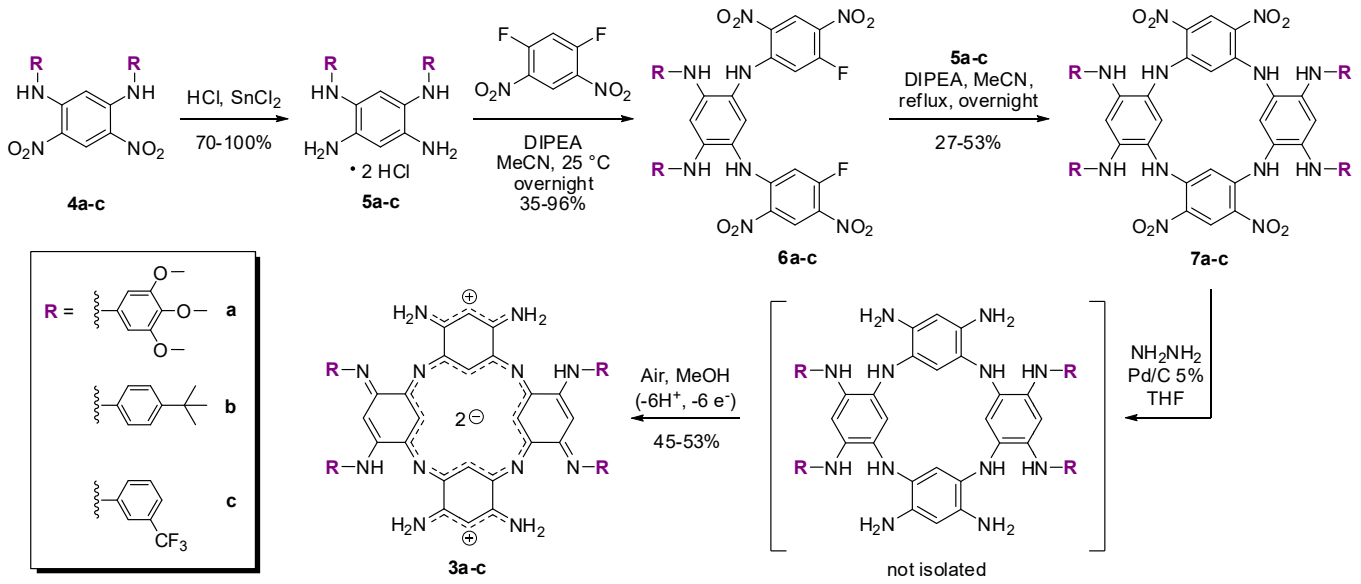

Scheme 1. Synthetic route to ACPs **3a-c**.

Herein, we report the synthesis of new *N*-aryl substituted azacalixphyrins and the study of their absorption properties. Their potential as PA contrast agent is investigated and shows a strong response upon NIR laser excitation. To the best of our knowledge, these results demonstrate that ACPs are the most red-shifted PA organic probes reported to date.

N-aryl substituted azacalixphyrins were designed following a synthetic pathway similar to *N*-alkyl analogues.[10c] First, *N,N*-substituted tetraaminobenzene hydrochloride intermediates **5a-c** were synthesized as described in the literature,[12] and then mixed with two equivalents of 1,5-difluoro-2,4-dinitrobenzene in presence of *N,N*-diisopropylethylamine (DIPEA) to afford adducts **6a-c**. These latter were engaged in nucleophilic aromatic substitutions with salts **5a-c** in refluxing acetonitrile to form symmetrical *N*-substituted azacalixarenes **7a-c**. Eventually, the four nitro groups of this series of macrocycles were reduced in presence of hydrazine monohydrate and Pd/C under heating to reach the corresponding colourless octaamino-azacalix[4]arene intermediates (not isolated) that spontaneously oxidize to the corresponding ACP series **3a-c** under aerobic conditions. Noteworthy, unlike compounds **1** and **2**, aryl-substituted macrocycles **3a-c** could be purified through flash column chromatography on alumina due to a relatively good solubility in polar organic solvents. Macrocycles **3a-c** were fully characterized exhibiting for instance a shielded chemical shift for the inner C-H protons (δ *ca*. –1.00 to –2.40 ppm) indicating the aromatic character of the central ring

Electronic absorption spectra of ACPs were then recorded in acidic and basic DMSO solutions‡ (see Table S1 and Fig. S20† for additional data in MeOH and DMF) and display, in all instances, panchromatic absorption with two distinct bands in the red and NIR regions. As a reference, the unsubstituted macrocycle **1•2H$^+$** in acidic DMSO exhibits a maximum at 882 nm (ε^{882} = 7200 $M^{-1}cm^{-1}$, Fig. 2).

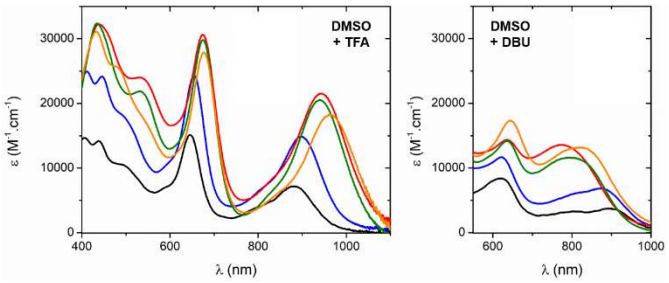

Fig. 2. Vis-NIR electronic absorption spectra of ACPs **1** (—), **2** (—), **3a** (—), **3b** (—) and **3c** (—) in acidic or basic DMSO.

As anticipated, upon peripheral substitution with octylamine moieties, a slight redshift is recorded for compound **2•2H$^+$** (λ_{max} = 897 nm), along with a significant hyperchromic effect (ε^{897} = 14900 $M^{-1}cm^{-1}$). Substitution with aryl moieties within ACP series

3a-c•2H$^+$ resulted in a marked bathochromic shift with absorption maxima now centred at *ca*. 940-960 nm, and with larger molar extinction coefficients in the range of 18000-22000 $M^{-1}cm^{-1}$. Such behaviour has been recently predicted for the diprotonated species by a theoretical approach which highlighted that, independently of the their electron-donating or electron-withdrawing nature, phenyl rings tend to redshift the absorption maxima thanks to enhancement of π-electrons delocalization.[13] In presence of DBU, all the neutral species (*i.e.* zwitterion species) are characterized by hypochromic shifts of both the red and NIR absorptions (Fig. 2). For **1** and **2**, the absorption maxima are less impacted, whereas for aryl-substituted dyes **3a-c**, the neutral species showed a noticeable blueshift of their lower energy transition towards 800 nm. Such hypsochromic effects can be correlated to theoretical data which predicted that, as illustrated in Fig. 1, amines bearing aromatic substituents (**3a-c**) should stabilize tautomer of the macrocycle that differs from alkyl-substituted one (**2**), the peripheral cationic cyanine being found on the unsubstituted trimethine units.[13] For the records, the TD-DFT data and key molecular orbitals involved in the **2H$^+$** forms of the investigated dyes can be found in the ESI† as well (Figs. S30-S32†).

The acido-basic properties and absorption pH-dependence (Fig. S21†) of ACP **3a** (2.4 < pH < 11.6) were then investigated in a mixture of MeOH/H_2O (80/20 *w/w*). Under acidic conditions, **3a•2H$^+$** is characterized by a strong absorption centred at 671 nm (ε^{671} = 24700 $M^{-1}cm^{-1}$) and an apparent tail of the intense NIR absorption (*i.e.* not measured due to instrumental limitations) in agreement with data recorded in other solvents such as DMSO, DMF or MeOH (Fig. 2, Fig. S20 and Table S1†). Upon pH increase, the visible absorption faded as a consequence of the deprotonation of the two aryl-substituted cationic cyanine subunits (Figs. S21-S25†). For the neutral **3a** species (*i.e.* zwitterion), significant hypsochromic and hypochromic shifts of the NIR band to ca. 775 nm (ε^{775} ~ 10100 $M^{-1}cm^{-1}$) were measured in agreement with related data (Fig. S20 and Table S1†). Two basic pK_a values (pK_{a1} = 9.9(4) and pK_{a2} = 11.5(3)) were calculated following statistical processing of the absorption and potentiometric data sets. Such behaviour was already evidenced for the reference compound **1** (pK_{a1} = 12.50(5) and pK_{a2} = 15.21(3) in DMSO/H_2O 80/20 *w/w*).[14] The aryl-substituted cationic trimethines are stabilized over a much broader pH range when compared to the *N*-arylated quinonediimine model[13] (pK_a = 8.1(1)). As a result, we thus anticipate that the diprotonated species **3a•2H$^+$** predominates at physiological pH, a major requirement for potential use of ACP for PAI.

The PA response of a contrast agent is directly correlated to its local absorption, surrounding medium and spatial orientation from the incident laser beam illuminating the zone of interest. The amplitude of the time-resolved PA signal is controlled by the initial generated pressure P_0, source of the acoustic response, directly proportional to the optical fluence locally deposited: $P_0 = \Gamma\mu_a(\lambda)\varphi(\lambda)$ (see the ESI† for details). The absorption coefficient $\mu_a(\lambda)$ of the solution is related to the vis-NIR electronic absorption measurements (Fig. 2) and the initial concentration *c*, as follows: $\mu_a=\varepsilon(\lambda)c$. Hence, knowing the physics of propagation of optical and acoustic waves in the investigated medium, one can reconstruct the absorption coefficient. According to the molecules size (< 1 nm), one can assume that the total extinction is equal to absorption (no scattering), and the fluence can be determined using the Beer-Lambert's law $\varphi=\varphi_0 e^{-\mu_a z}$, φ_0 being the input light fluence, and *z* the depth at which the medium is probed.

To evaluate the potential of ACPs as PA contrast agent, an experimental setup was built (see Fig. S26† for details) and ACPs were introduced in a flexible and transparent polymeric tube (TYGON®R-3603, Saint Gobain) with an inner diameter of 1 mm, chosen to avoid any additional acoustic contrast. The tube was immersed in a water tank for acoustic coupling and scanned in a 4×4 mm zone with a step size of 0.1 mm, identical in both x- and y-axis. From the set of 2D scanning measurements, images of the maximum intensity PA (MIP) signal were obtained with a high contrast for ACP **3a** (Fig. 3). To highlight the impact of the *N*-substituents, spectroscopic measurements were then performed by tuning the laser wavelength from 700 to 1000 nm for three dyes (**1**, **2**,and **3a**) in two different solvents (*i.e.* MeOH and DMSO, Fig. 4 and S28†) in an OptiCell™ chamber. Importantly, the dual plot of the measured PA amplitudes *vs*. the electronic absorption spectra in MeOH show that the fluctuations in the measured PA signal are unambiguously representative of the corresponding absorption spectra of the ACP dyes in the same solvent.‡‡ A synthetic visualization of the normalized MIP obtained from different ACP molecules in both solvents is depicted in Fig. 5. This normalized PA response of the three macrocycles is a direct measurement of the absorption coefficient, from which the molecular extinction coefficient can be obtained, and allows choosing the most efficient contrast agent for a given wavelength. While alkyl-substituted ACP **2** exhibits an intense response at *ca*. 900 nm in both solvents, the PA signal recorded for ACP **3a** was found to be moderate in DMSO. However in MeOH, the aryl-substituted macrocycle being diprotonated (**3a•2H$^+$**) featured the strongest PA response within the 800-1000 nm range. Such broad spectral coverage is particularly useful since various excitation wavelengths within the NIR-I transparency window can be selected.

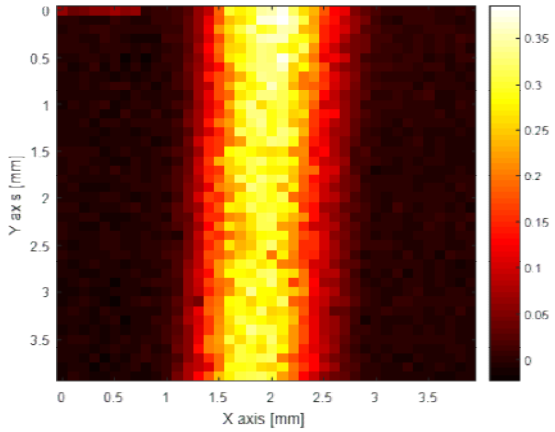

Fig. 3. Reconstructed image of the MIP response [AU] of a tube filled with ACP **3a** in MeOH (*ca*. 100 µM) measured at 938 nm.

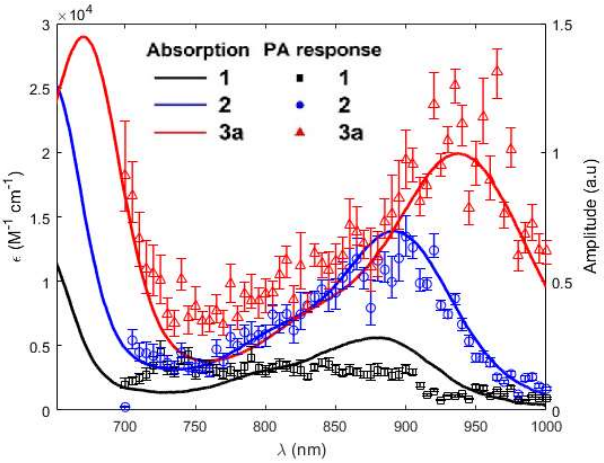

Fig. 4. Vis-NIR electronic absorption spectra of **1** (—), **2** (—) and **3a** (—) compared to PA amplitude measurements of ACPs **1** (■), **2** (●), **3a** (▲) in MeOH (*ca*. 100 µM).

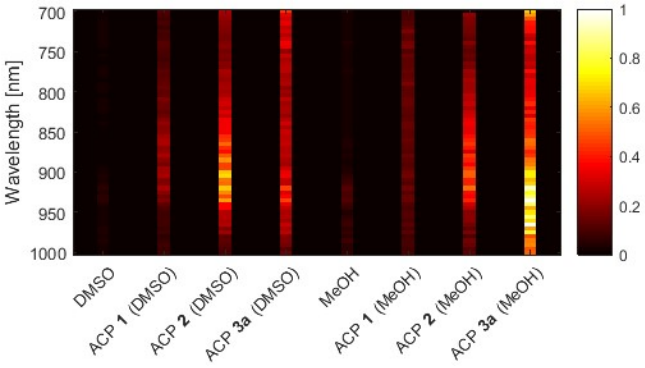

Fig. 5. Global visualization of all spectroscopic MIP measurements in solution (*ca*. 100 µM), normalized to the maximum amplitude of all acquired signals (*i.e.*, PA signal of **3a** in MeOH at 935 nm).

In conclusion, we successfully synthesized a series of aryl-substituted azacalixphyrin macrocycles featuring an absorption bathochromic effect with respect to alkyl-substituted analogues, with absorption maxima lying beyond 900 nm. In addition, this aryl-substitution confers a good solubility in highly polar solvents and pH-dependent absorption highlighted the predominant formation of NIR-absorbing diprotonated species beyond pH 10 in protic environment. The evaluation of the PA response upon NIR laser excitation confirmed the generation of ultrasounds, with an amplitude depending on the absorption coefficient of the dyes, thus allowing the use of selected excitation wavelengths within the NIR transparency region. Henceforth, future investigations will be focused on the use of ACPs as *in vivo* PA probes for bio-imaging.

This work was supported by the Centre National de la Recherche Scientifique, the Ministère de la Recherche et des Nouvelles Technologies (PhD grant to Z.C.) and the Agence Nationale de la Recherche in the frame of the EMA project (PhD grant to L.L.).

Notes and references

‡ The nature of the solvent has a strong influence on the absorption profiles (see Fig. S20†) which is mainly due to the mixture of different protonated species in solution. Thus, 0.1 M trifluoroacetic acid (TFA) or 0.1 M 1,8-diazabicyclo[5.4.0]undec-7-ene (DBU) were added to the solutions to ensure the presence of neutral and diprotonated species, respectively. The strong impact of the presence of water in the solvent is also illustrated in Figure S28†.
‡‡ Care was taken to confirm the linearity of the PA response depending on the concentration of the chromophore in solution for ACP **3a** between 100 and 2 µM in MeOH and DMSO (Fig. S29†).

1 (a) M. Xu and L. V. Wang, *Rev. Sci. Instrum.*, 2006, **77**, 041101; (b) L. V. Wang and S. Hu, *Science*, 2012, **335**, 1458; (c) V. Gujrati, A. Mishra and V. Ntziachristos, *Chem. Commun.*, 2017, **53**, 4653.

2 (a) K. S. Valluru, K. E. Wilson and J. K. Willmann, *Radiology*, 2016, **280**, 332-349; (b) S. Zackrisson, S. M. W. Y. van de Ven and S. S. Gambhir, *Cancer Res.*, 2014, **74**, 979.

3 (a) S. A. Ermilov, T. Khamapirad, A. Conjusteau, M. H. Leonard, R. Lacewell, K. Mehta, T. Miller and A. A. Oraevsky, *J. Biomed. Opt.*, 2009, **14**, 0.4007; (b) M. Heijblom, D. Piras, W. Xia, J. C. G. van Hespen, J. M. Klaase, F. M. van den Engh, T. G. van Leeuwen, W. Steenbergen and S. Manohar, *Opt. Express*, 2012, **20**, 11582.

4 (a) D. Razansky, C. Vinegoni and V. Ntziachristos, *Opt. Lett.*, 2007, **32**, 2891-2893; (b) L. Changhui and V. W. Lihong, *Phys. Med. Biol.*, 2009, **54**, R59.

5 H. F. Zhang, K. Maslov and L. V. Wang, *Nat. Protoc.*, 2007, **2**, 797.

6 X. Wang, Y. Pang, G. Ku, X. Xie, G. Stoica and L. V. Wang, *Nat. Biotechnol.*, 2003, **21**, 803.

7 (a) L. Nie and X. Chen, *Chem. Soc. Rev.*, 2014, **43**, 7132; (b) J. Weber, P. C. Beard and S. E. Bohndiek, *Nat. Methods*, 2016, **13**, 639; (c) C. J. Reinhardt and J. Chan, *Biochemistry*, 2018, **57**, 194.

8 (a) M. Frenette, M. Hatamimoslehabadi, S. Bellinger-Buckley, S. Laoui, J. La, S. Bag, S. Mallidi, T. Hasan, B. Bouma, C. Yelleswarapu and J. Rochford, *J. Am. Chem. Soc.*, 2014, **136**, 15853; (b) H. Li, P. Zhang, L. P. Smaga, R. A. Hoffman and J. Chan, *J. Am. Chem. Soc.*, 2015, **137**, 15628; (c) P. Anees, J. Joseph, S. Sreejith, N. V. Menon, Y. Kang, S. Wing-Kwong Yu, A. Ajayaghosh and Y. Zhao, *Chem. Sci.*, 2016, **7**, 4110; (d) K. Miki, A. Enomoto, T. Inoue, T. Nabeshima, S. Saino, S. Shimizu, H. Matsuoka and K. Ohe, *Biomacromolecules*, 2017, **18**, 249; (e) H. Xiao, C. Wu, P. Li, W. Gao, W. Zhang, W. Zhang, L. Tong and B. Tang, *Chem. Sci.*, 2017, **8**, 7025; (f) B. Shi, X. Gu, Q. Fei and C. Zhao, *Chem. Sci.*, 2017, **8**, 2150; (g) M. Hatamimoslehabadi, S. Bellinger, J. La, E. Ahmad, M. Frenette, C. Yelleswarapu and J. Rochford, *J. Phys. Chem. C*, 2017, **121**, 24168; (h) B. Stephanie, H. Maryam, B. Seema, M. Farha, L. Jeffrey, F. Mathieu, L. Samir, S. D. J., Y. Chandra and R. Jonathan, *Chem. Eur. J.*, 2018, **24**, 906; (i) C. J. Reinhardt, E. Y. Zhou, M. D. Jorgensen, G. Partipilo and J. Chan, *J. Am. Chem. Soc.*, 2018, **140**, 1011; (j) S. Bellinger, M. Hatamimoslehabadi, R. E. Borg, J. La, P. Catsoulis, F. Mithila, C. Yelleswarapu, J. Rochford, *Chem. Commun.*, 2018, 54, 6352.

9 (a) I. T. Ho, J. L. Sessler, S. S. Gambhir and J. V. Jokerst, *Analyst*, 2015, **140**, 3731; (b) A. B. E. Attia, G. Balasundaram, W. Driessen, V. Ntziachristos and M. Olivo, *Biomed. Opt. Express*, 2015, **6**, 591; (c) N. Bézière and V. Ntziachristos, *J. Nucl. Med.*, 2015, **56**, 323; (d) S. Banala, S. Fokong, C. Brand, C. Andreou, B. Krautler, M. Rueping and F. Kiessling, *Chem. Sci.*, 2017, **8**, 6176; (e) H. D. Lu, T. L. Lim, S. Javitt, A. Heinmiller and R. K. Prud'homme, *ACS Comb. Sci.*, 2017, **19**, 397.

10 (a) Z. Chen, M. Giorgi, D. Jacquemin, M. Elhabiri and O. Siri, *Angew. Chem. Int. Ed.*, 2013, **52**, 6250; (b) G. Marchand, A. D. Laurent, Z. Chen, O. Siri and D. Jacquemin, *J. Phys. Chem. A*, 2014, **118**, 8883; (c) Z. Chen, R. Haddoub, J. Mahé, G. Marchand, D. Jacquemin, J. Andeme Edzang, G. Canard, D. Ferry, O. Grauby, A. Ranguis and O. Siri, *Chem. Eur. J.*, 2016, **22**, 17820; (c) C. Azarias, S. Pascal, O. Siri, D. Jacquemin, *Phys. Chem. Chem. Phys.*, 2018, **20**, 20056.

11 (a) S. Dähne and D. Leupold, *Angew. Chem. Int. Ed.*, 1966, **5**, 984; (b) O. Siri, P. Braunstein, M.-M. Rohmer, M. Bénard and R. Welter, *J. Am. Chem. Soc.*, 2003, **125**, 13793; (c) S. Pascal, L. Lavaud, C. Azarias, G. Canard, M. Giorgi, D. Jacquemin and O. Siri, *Mater. Chem. Front.*, 2018, **2**, 10186.

12 L. Lavaud, Z. Chen, M. Elhabiri, D. Jacquemin, G. Canard and O. Siri, *Dalton Trans.*, 2017, **46**, 12794.

13 G. Marchand, O. Siri and D. Jacquemin, *Phys. Chem. Chem. Phys.*, 2016, **18**, 27308.

14 G. Marchand, P. Giraudeau, Z. Chen, M. Elhabiri, O. Siri, D. Jacquemin, *Phys. Chem. Chem. Phys.* 2016**, *18***, 9608.